The Effect of Oxidation and Reduction of Chlorophyll *a* on Its Geometry, Vibrational and Spin Density Properties as Revealed by Hybrid Density Functional Methods

Patrick J. O'Malley*

Contribution from the Department of Chemistry, UMIST, Manchester, M60 1QD, UK

Received April 13, 2000

Abstract: The oxidation and reduction of a chlorophyll *a* model molecule is investigated using hybrid density functional, B3LYP, calculations. The geometry, vibrational modes, and spin density distributions of the free radical forms are investigated. Small bond length changes on oxidation or reduction are shown to lead to significant variations in certain vibrational mode frequency values. Bond length changes can be readily accounted for by the electron density distributions of the frontier HOMO and LUMO orbitals. Harmonic frequency shifts calculated for oxidation and reduction on the 13^1CO stretching frequency show very good agreement with experimental determinations. The unpaired spin density distribution for the cation and anion free radicals is also computed, and calculated ^{14}N and ^{25}Mg isotropic hyperfine coupling constants are in good agreement with experiment.

Introduction

In the initial photochemistry associated with light energy transduction by the Photosystem I (PS I) reaction center of cyanobacteria, algae, and green plants, light energy is used to initiate electron transfer between neighboring chlorophyll *a* molecules.[1] Two initially neutral ground-state chlorophyll *a* molecules are transformed by the electron-transfer reaction into chlorophyll *a* cation and anion free radicals. In photosystem II and bacterial photosynthesis a similar charge separation occurs. To understand the mechanism of charge separation extensive use has been made of spectroscopic techniques such as electron paramagnetic resonance (EPR) and Fourier transform infrared (FTIR) spectroscopy.[2−5] The formation of the free radicals can be detected by the characteristic EPR signal of the cation or anion free radical formed. Here hyperfine coupling data can be of particular use in probing the electronic structure of the free radicals. FTIR difference spectroscopy can be used to probe both the ground state and free radical forms. Here changes in the frequencies of vibrational bands can be used to monitor oxidation and reduction. Both techniques together with optical techniques have been widely used to monitor the initial charge separation in photosynthetic reaction centers. Because of the complexity of the systems involved often only partial information is obtained from both techniques. As such assignment of hyperfine couplings to specific interactions or assignment of FTIR bands to specific vibrational modes is difficult. While in vitro model compound studies can be of help there is a need for an in depth understanding of the changes in both the frequencies and intensities of the vibrational bands as the molecule is transformed into its free radical forms via oxidation or reduction. In such cases the availability of accurate predicted data from high level electronic structure methods would be particularly valuable. Until recently the applicability of accurate electronic structure methods, which include electron correlation, to molecules the size of chlorophyll has been prohibitive in terms of cost. This is especially the case for the calculation of optimized geometries and harmonic frequencies. The development in recent years of density functional methods has been particularly significant in this regard.[6,7] Because of their favorable computational cost they are increasingly applied to ever larger molecules and free radicals. In particular hybrid type methods which partially include some Hartree−Fock exchange have proved particularly accurate in predicting the properties of both closed and open shell molecules.[8,9]

Here we now demonstrate how such methods can be used to predict the changes in vibrational band frequencies and intensities of the chlorophyll molecule that occur on oxidation and reduction. Direct experimental and theoretical comparison can be made between the effect of oxidation and reduction on the carbonyl stretching frequency for the 13^1 position. The predicted changes are shown to be in in excellent agreement with the changes derived from FTIR studies. Significant changes in relative intensities of IR bands are predicted to occur in the different states and may need to be taken into account in experimental assignments. Isotropic hyperfine couplings calculated for the ^{14}N and ^{25}Mg nucleus for the free radical forms are shown to be in good agreement with experimental measurement.

Methods

The model of chlorophyll *a* used is shown in Figure 1. All geometry optimizations and harmonic frequency calculations were performed

(1) Brettel, K. *Biochim. Biophys. Acta* **1997**, *1318*, 322−342.
(2) Norris, J. R.; Uphaus, R. A.; Crespi, H. L.; Katz, J. *Proc. Natl. Acad. Sci. U.S.A.* **1971**, *71*, 625−628.
(3) O'Malley, P. J.; Babcock, G. T. *Proc. Natl. Acad. Sci. U.S.A.* **1984**, *81*, 1098−1101.
(4) Breton, J.; Nabedryk, E.; Leibl, W. *Biochemistry* **1999**, *38*, 11585−11592.
(5) Nabedryk, E.; Leonhard, M.; Mantele, W.; Breton, J. *Biochemistry* **1990**, *29*, 3242−3247
(6) Kohn, W. *Rev. Mod. Phys.* **1999**, *71*, 1253−1266.
(7) Becke, A. D. J. *Chem. Phys.* **1993**, *98*, 5648−5652.
(8) Barone, V. In *Recent Advances in Density Functional Methods*; Chong, D. P., Ed.; World Scientific Publishing: Singapore, 1995. (b) Rega, N.; Cossi, M.; Barone, V. *J. Am. Chem. Soc.* **1998**, *120*, 5723.
(9) O'Malley, P. J.; Collins, S. J. *Chem. Phys. Lett.* **1996**, *259*, 296−300. (b) O'Malley, P. J. *Chem. Phys. Lett.* **1996**, *262*, 797−801.

10.1021/ja001284q CCC: $19.00
Published on Web 07/26/2000

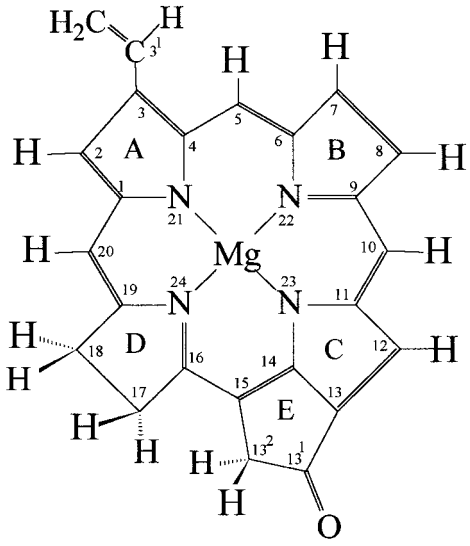

Figure 1. Model of chlorophyll *a* and numbering system used.

Table 1. Selected Optimized Bond Lengths (Å) for the Chlorophyll *a* Model of Figure 1[a]

bond	anion	neutral	cation	bond	anion	neutral	cation
Mg−N21	2.048	2.030	2.023	C11−C12	1.423	1.443	1.467
Mg−N22	2.074	2.072	2.065	C12−C13	1.411	1.386	1.369
Mg−N23	2.037	2.020	2.016	C13−C14	1.416	1.425	1.438
Mg−N24	2.141	2.154	2.142	C14−C15	1.424	1.413	1.396
C1−C2	1.415	1.437	1.441	C15−C16	1.370	1.378	1.399
C2−C3	1.399	1.377	1.370	C16−C17	1.510	1.519	1.522
C3−C4	1.445	1.463	1.484	C17−C18	1.540	1.544	1.543
C4−C5	1.411	1.391	1.395	C18−C19	1.517	1.525	1.529
C5−C6	1.397	1.413	1.409	C19−C20	1.375	1.388	1.392
C6−C7	1.449	1.442	1.459	C13−C13[1]	1.452	1.473	1.498
C7−C8	1.365	1.370	1.358	C13[1]−C13[2]	1.574	1.569	1.567
C8−C9	1.450	1.441	1.459	C13[2]−C15	1.523	1.524	1.525
C9−C10	1.397	1.406	1.402	C13[1]−O	1.229	1.216	1.208
C10−C11	1.417	1.398	1.403				

using standard procedures of Gaussian 98.[10] The B3LYP functional was used throughout in combination with the 6-31G(d) basis set. Unrestricted Kohn−Sham was used for the radical forms. Absolute values of computed harmonic frequencies should not be compared directly with experimental anharmonic values. At this level of theory computed harmonic frequencies can be expected to overestimate experimental anharmonic values by approximately 5%. In this report we are concerned with *differences* in frequency values where, assuming anharmonic contributions are constant, valid comparison can be made between computed frequency shifts and experimental determinations.

Results and Discussion

A representative sample of bond distances optimized for the cation, neutral, and anion states are given in Table 1.

Small but significant changes in bond lengths are noted on going from the cation to the neutral through to the anion state. In general the variations in bond lengths can be correlated with the occupancy of the frontier HOMO/LUMO orbitals. The electron density contours for the HOMO and LUMO are illustrated in Figure 2 and as an illustration of the above correlation we take the bond lengths in ring A as an example.

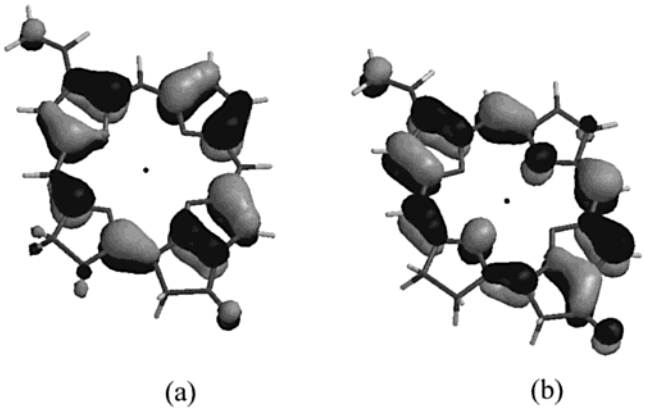

Figure 2. HOMO(a) and LUMO(b) electron density, 0.03e/au^3, contour plots for the neutral molecule of Figure 1. Orientation of molecules is as shown in Figure 1.

Table 2. Calculated Harmonic Frequencies (cm^{-1}) and IR Intensities (km/mol) (in brackets), for the Chlorophyll *a* Model of Figure 1

mode form	neutral	cation	anion
13[1]C−O stretch	1806(717)	1832(423)	1747(1549)
vinyl stretch	1701(3)	1683(64)	1677(302)
ring stretch (C15−C16), (C19−C20)	1660(264)	1639(316)	1675(171)

Table 1 shows that the C1−C2 and C3−C4 bond lengths decrease in going from the cation to the anion form. The HOMO orbital is bonding for both bonds and hence explain the decreased bond length on going from cation (singly occupied) to neutral(doubly occupied). The additional electron in the anion form occupies an orbital, Figure 2b, which is also bonding between for these two bonds and hence a further decrease in bond length is found. The C2−C3 bond length, on the other hand, behaves oppositely to the above, that is, an increase in bond length is observed in going from cation to the anion form. Here, both the HOMO and LUMO are antibonding for the C2−C3 bond. Similar correlations can be put forward to explain most of the bond length variations exhibited in Table 1.

Of particular note is the progressive increase in C−O bond distance of the 13[1] carbonyl in going from the cation to the anion state. This group is an important marker used in difference FTIR studies where the frequency of the intense CO stretching mode has been used to monitor oxidation and reduction.[4,5] The changes in the calculated harmonic frequency of this mode are given for each state in Table 2. On oxidation to form the cation radical the mode frequency is predicted to shift in frequency by +26 cm^{-1} in excellent agreement with the experimentally reported shift of +25 cm^{-1} for chlorophyll *a* in tetrahydrofuran-(THF).[5] Reduction to form the anion free radical results in a predicted shift of −59 cm^{-1} which again compares very favorably with the experimental shifts of −50 cm^{-1}.[11] These shifts in frequency for the CO stretching frequency reflect the change in bond order of the 13[1]CO bond in the various oxidation states. This is shown by the CO bond lengths of Table 1 where there is a progressive decrease in the CO bond length in going from anion to the cation. These variations can be related to the occupancy of the frontier HOMO/LUMO orbitals, Figure 2, for each oxidation state. In the cation state the HOMO, Figure 2a

(10) Frisch, M. J.; Trucks G. W.; Schlegel, H. B.; Gill, P. W.; Johnson, B. G.; Wong, M. W.; Foresman, J. B.; Tomasi, J.; Barone, V.; Adamo, C.; Robb, M. A.; Head-Gordon, M.; Replogle, E. S.; Gomperts, R.; Andres, J. L.; Raghvachari, K.; Binkley, J. S.; Gonzalez, C.; Martin, R. L.; Fox, D. J.; Defrees, D. J.; Baker, J.; Gonzalez, C.; Martin, R. L.; Fox, D. J.; Defrees, D. J.; Baker, J.; Stewart, J. J. P.; Pople, J. A. *Gaussian 98*; Gaussian Inc.: Pittsburgh, PA, 1998.

(11) Nabedryk, E.; Andrianambinintsoa, S.; Berger, G.; Leonhard, M.; Mantele, W.; Breton, J. *Biochim. Biophys. Acta* **1990**, *1016*, 49−54. (b) Mantele, W.; Wollenweber, A.; Rashwan, F.; Heinze, J.; Nabedryk, E.; Berger, G.; Breton, J. *Photochem. Photobiol.* **1988**, *47*, 451−455

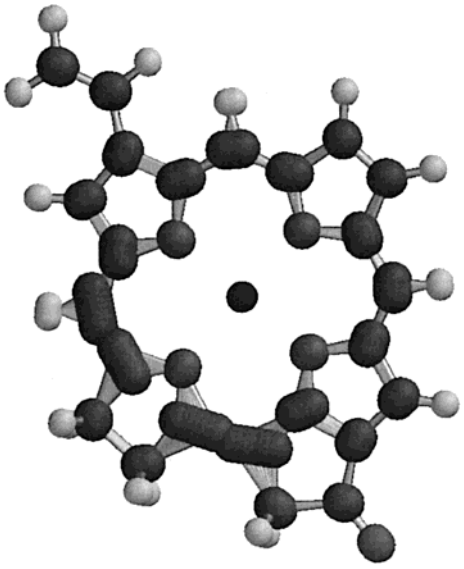

Figure 3. Seven frames illustrating the C15−C16 and C19−C20 ring stretching vibrational mode. Orientation of molecule is as shown in Figure 1.

is singly occupied. The HOMO is antibonding between the atoms C13[1] and O and double occupancy in the neutral state can therefore be expected to lead to a reduction in the 13[1]CO bond order, leading to the increase in bond length and a decrease in stretching frequency as noted above on going from the cation to the neutral state. On reduction to form the anion state the extra electron occupies the LUMO orbital shown in Figure 2b. This orbital is strongly antibonding between the 13[1]C and oxygen atom and hence a further decrease in bond order can be expected for 13[1]CO in the anion state leading to the increase in bond length and reduction in stretching frequency observed. The effect of ^{13}C isotope substitution on the 13[1]CO stretching vibration has also been studied for the ground-state chlorophyll *a* molecule. A shift of −44 cm^{-1} has been reported.[12a] Our predicted shift is −46 cm^{-1}, in excellent agreement with the experimental determination.

Table 2 also shows the change in frequency and intensity occurring for two other high-frequency modes of the chlorophyll model. These modes correspond to the vinyl stretch and a ring stretching mode observed in previous experimental studies of the neutral state.[12] This table serves not only to illustrate the significant frequency shifts observed for these modes but also the significant intensity changes predicted to occur on either oxidation or reduction. Previous assignments for the cation state in vitro may need to be reassessed based on these findings.[13] The mode form of the highest frequency ring stretch is illustrated in Figure 3. This mode involves predominantly asymmetric stretching of the C15−C16 and C19−C20 bonds. This mode corresponds to the infrared and Raman band observed in the region 1610−1597 cm^{-1} [12] and it has been used as a marker band for the coordination of Mg although this is the first time it has been specifically assigned to the C15−C16 and C19−C20 stretching vibrations. Other ring stretches appear at lower frequencies. The higher value observed for the C15−C16 and C19−C20 stretching mode can again be correlated with the shorter bond lengths of these two bonds, Table 1. This may be related to the fact that these bonds are neighbors to the reduced ring D which, for the HOMO orbital at any rate, leads to an increased electron density in these neighboring bonds, Figure 2a. Table 2 shows that the frequency value for this mode increases on going from the cation to the anion state. This trend again correlates with the corresponding decrease in bond length seen in Table 1. This in turn would appear to be related to the bonding nature of both the C15−C16 and C19−C20 bonds in both the HOMO and LUMO, Figure 2. Occupancy of the HOMO and LUMO can be predicted to increase both bond orders leading to decreased bond lengths and increased stretching vibrations as one proceeds from cation to anion state.

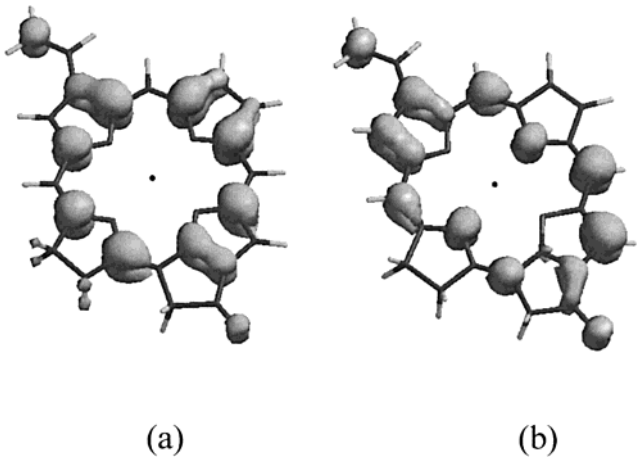

Figure 4. Unpaired spin density contours, 0.002 e/au^3, for (a) cation and (b) anion free radical forms of the chlorophyll *a* model of Figure 1. Orientation of radical is as shown in Figure 1.

Table 3. Calculated ^{25}Mg and ^{14}N Isotropic Hyperfine Coupling Constants for the Chlorophyll *a* Model of Figure 1[a]

position	anion	cation
Mg	0.8(0.9)	−0.4(−0.3)
N21	−1.6(−2.0)	−2.1(−2.1)
N22	5.3(4.4)	−3.5(−3.2)
N23	−0.8(−0.6)	−2.1(−2.4)
N24	6.5(5.5)	−2.4(−2.7)

[a] Experimental values[14,15] are given in brackets. All values given in MHz.

In Figure 4 the unpaired spin density contours for the cation and anion free radical forms are illustrated. As expected they mirror the HOMO/LUMO contours of Figure 2. The anion spin density distribution is similar to that recently described for the larger pheophytin model.[16] In Table 3 the predicted isotropic hyperfine couplings for the ^{14}N and ^{25}Mg nuclear hyperfine interaction are presented and compared with experimental determinations for chlorophyll-type radicals. The agreement between predicted and experimental couplings is very impressive. Previous studies on other organic radicals have already demonstrated the predictive capabilities for hyperfine coupling prediction for ^{1}H, ^{13}C, and ^{14}N.[16] Here we show that equally impressive predictions are made for the ^{25}Mg nucleus as well.

Conclusions

It has therefore been demonstrated that hybrid density functional methods, B3LYP, are capable of accurately predicting the changes in vibrational mode frequencies that occur when

(12) Sashima, T.; Abe, M.; Kurano, N.; Miyachi, S.; Koyama, Y. J. *Phys. Chem. B* **1998**, 6903−6914.(b)Fujiwara, M.; Tasumi, M. *J. Phys. Chem.* **1986**, *90*, 5646−5650.

(13) Heald, R. L.; Cotton, T. M. *J. Phys. Chem.* **1990**, *94*, 3968−3975.

(14) Lubitz, W. Chlorophylls. In *CRC Handbook*; Scheer, H., Ed.; CRC Press: Boca Baton, FL, 1991; pp 903−944.

(15) Lendzian, F.; Mobius, K.; Plato, M.; Smith, U. H.; Thurnauer, M. C.; Lubitz, W. *Chem. Phys. Lett.* **1984**, *111*, 583−586.

(16) O'Malley, P. J. *J. Comput. Chem.* **1999**, *20*, 1292−1298. (b) O'Malley, P. J. *J. Phys. Chem. B* **2000**, *104*, 2176−2182.

chlorophyll *a* is one-electron oxidized or reduced. Isotropic hyperfine couplings are also impressively predicted for the free radicals. Recent work has demonstrated the ability of time-dependent density functional-based methods to accurately predict the electronic spectra of chlorophyll *a*.[17] While most of the calculations performed so far have been performed on model compounds in the gas phase, extension of such calculations to the condensed phase and indeed to the simulation of the immediate protein environment is now becoming feasible using continuum models[18] and layer-type calculations,[19] respectively. The future combination of such calculations with optical, vibrational and magnetic resonance spectroscopic techniques is likely to prove particularly fruitful in providing an electronic level understanding of photosynthetic electron transfer.

JA001284Q

(17) Sundholm, D. *Chem. Phys. Lett.* **2000**, *317*, 545−552.
(18) Cramer, C. J.; Truhlar, D. G. *Chem. Rev.* **1999**, *99*, 2161.
(19) Karadakov, P. B.; Morokuma, K. *Chem. Phys. Lett.* **2000**, *317*, 589−596.